

A Robust Ensemble-based Data Assimilation Method using Shrinkage Estimator and Adaptive Inflation

Santiago Lopez-Restrepo¹, Elias David Nino Ruiz², Andres Yarce Botero³, Luis G Guzman-Reyes², O. Lucia Quintero Montoya³, Nicolas Pinel³, Arjo Segers⁴, and Arnold Heemink⁵

¹Delft University of Technology

²Universidad del Norte

³Universidad EAFIT

⁴TNO

⁵Delft University of Technology

November 26, 2022

Abstract

This work proposes a robust and non-gaussian version of the shrinkage-based EnKF implementation, the EnKF-KA. The proposed method is based in the robust H filter and in its ensemble time-local version the EnTLHF, using an adaptive inflation factor depending on the shrinkage covariance estimated matrix. This implies a theoretical and solid background to construct robust filters from the well-known covariance inflation technique. The method is tested using the Lorenz-96 model to evaluate the robustness and performance under different scenarios as ensemble size, observation error, errors in the model specifications, and ensemble gaussianity. The results suggest good robustness of the proposed method in all the evaluated cases compared with the standard EnKF, the shrinkage-based EnKF-KA, and the robust EnTLHF.

A Robust Ensemble-based Data Assimilation Method using Shrinkage Estimator and Adaptive Inflation

Santiago Lopez-Restrepo^{1,2,3}, Elias D. Nino-Ruiz⁴, Andres Yarce^{1,2,3}, Luis G.
Guzman-Reyes⁴, O. L. Quintero¹, Nicolás Pinel⁵, Arjo Segers⁶, A. W.
Heemink²

¹Universidad EAFIT, Mathematical Modelling Research Group, Medellín, Colombia

²Department of Applied Mathematics, TU Delft, The Netherlands

³SimpleSpace, Medellín, Colombia

⁴Universidad del Norte, Applied Math and Computer Science Laboratory, Department of Computer
Science, Barranquilla, Colombia

⁵Universidad EAFIT, Grupo de Investigación en Biodiversidad Evolución y Conservación (BEC),

Departamento de Ciencias Biológicas, Medellín, Colombia

⁶Department of Climate, Air and Sustainability, TNO, The Netherlands

Key Points:

- A robust ensemble based estimation is proposed
- Adaptive inflation for the proposed filter is derived
- Theoretical development of both the robust filter and adaptation scheme is presented

Corresponding author: Santiago Lopez-Restrepo, s.lopezrestrepo@tudelft.nl,
slopezr2@eafit.edu.co

19 **Abstract**

20 This work proposes a robust and non-gaussian version of the shrinkage-based EnKF im-
 21 plementation, the EnKF-KA. The proposed method is based in the robust H_∞ filter and
 22 in its ensemble time-local version the EnTLHF, using an adaptive inflation factor de-
 23 pending on the shrinkage covariance estimated matrix. This implies a theoretical and
 24 solid background to construct robust filters from the well-known covariance inflation tech-
 25 nique. The method is tested using the Lorenz-96 model to evaluate the robustness and
 26 performance under different scenarios as ensemble size, observation error, errors in the
 27 model specifications, and ensemble gaussianity. The results suggest good robustness of
 28 the proposed method in all the evaluated cases compared with the standard EnKF, the
 29 shrinkage-based EnKF-KA, and the robust EnTLHF.

30 **Plain Language Summary**

31 Data assimilation is a mathematical process that combines two sources of informa-
 32 tion (models and observations) in an optimal way. In this work, we propose a new ro-
 33 bust ensemble-based data assimilation algorithm that allows the user to incorporate knowl-
 34 edge or dynamics that are not well represented by the model. Additionally, the proposed
 35 algorithm is suitable for non-linear and non-gaussian problems with a scarce error char-
 36 acterization. We evaluate the algorithm using the Lorenz-96 model and compare its per-
 37 formance against other well-known ensemble-based data assimilation algorithm. The re-
 38 sults show that our propose can outperform the other methods reducing the estimation
 39 error and increasing the robustness.

40 **1 Introduction**

41 Data assimilation (DA) is a mathematical family of methods that allows the combi-
 42 nation of observations and models. The model is used to fill observational gaps, and
 43 the observations constrain the model dynamics (Lahoz & Schneider, 2014; Bocquet et
 44 al., 2015). In most of the DA methods, the aim is to minimize the estimated error vari-
 45 ance. For instance, Kalman Filter (KF) is an optimal method that minimizes the mean-
 46 squared-error in the estimation. The KF is optimal when the following assumptions are
 47 fulfilled: the dynamic system is linear, and the observation and model uncertainties fol-
 48 low a Gaussian distribution (Kalman, 1960). The Ensemble Kalman Filter (EnKF) is
 49 a KF-based Monte carlo approximation of the KF when the state space is large, and the
 50 model is non-linear (Evensen, 2003). The EnKF uses an ensemble of model realization
 51 to approximate the first and second background error moments, making it efficient for
 52 large-scale models and suitable in the presence of non-linearities. However, in real DA
 53 applications, the assumptions required to obtain the optimal solution may not be accu-
 54 rate, degrading the filter performance (Houtekamer et al., 2005; Evensen, 2003). Addi-
 55 tionally, small ensemble sizes may produce a poor approximation of the model uncer-
 56 tainty, causing a reduction in the filter accuracy or even filter divergence.

57 When the system conditions do not satisfy the KF-based methods requirement, a
 58 different approach is a robust filter or robust estimator. The robust filters emphasize the
 59 robustness of the estimation to have better tolerances to high uncertainty sources. Since
 60 its purpose is not the optimality in the estimation, the robust estimator does not require
 61 a strictly statistical representation of the system and the observations (Luo & Hoteit,
 62 2011), showing a better performance than the KF-based methods in scenarios with a poor
 63 statistical uncertainty representation (Han et al., 2009; Nan & Wu, 2017). There are sev-
 64 eral robust ensemble-based DA schemes based in different aspect such as H_∞ formula-
 65 tion (Han et al., 2009), replacing the traditional L_2 norm (Roh et al., 2013; Freitag et
 66 al., 2013; Rao et al., 2017), robust covariance estimation (Yang et al., 2001; E. Nino-Ruiz
 67 et al., 2018), and covariance inflation (Luo & Hoteit, 2011; Bai et al., 2016). The approach
 68 that we propose uses a shrinkage-based covariance estimator that improves the model

69 robustness and performance when the ensemble size is small. Additionally, our method
 70 incorporates adaptive covariance inflation closely related to the H_∞ formulation.

71 2 Ensemble-Based Data Assimilation

72 In ensemble-based data assimilation, an ensemble of model realizations

$$73 \quad \mathbf{X}^b = [\mathbf{x}^{b[1]}, \mathbf{x}^{b[2]}, \dots, \mathbf{x}^{b[N]}] \in \mathbb{R}^{n \times N}, \quad (1)$$

74 is employed to estimate the first (\mathbf{x}^b) and second moments (\mathbf{B}) of the background error
 75 distributions, where $\mathbf{x}^{b[i]} \in \mathbb{R}^{n \times 1}$ is the i -th ensemble member, and N is the total number
 76 of ensemble members. Hence:

$$77 \quad \mathbf{x}^b \approx \bar{\mathbf{x}}^b = \frac{1}{N-1} \cdot \sum_{e=1}^N \mathbf{x}^{b[e]} \in \mathbb{R}^{n \times 1}, \quad (2)$$

78 and

$$79 \quad \mathbf{B} \approx \mathbf{P}^b = \frac{1}{N} \cdot \Delta \mathbf{X} \cdot \Delta \mathbf{X}^T \in \mathbb{R}^{n \times n}, \quad (3)$$

80 where

$$81 \quad \Delta \mathbf{X} = \mathbf{X}^b - \bar{\mathbf{x}}^b \cdot \mathbf{1}^T \in \mathbb{R}^{n \times N}, \quad (4)$$

82 is the anomalies matrix, $\bar{\mathbf{x}}^b$ is the ensemble mean, \mathbf{P}^b is the sample covariance matrix,
 83 and $\mathbf{1}$ is a vector with components all ones. Once an observation is available, the posterior
 84 state can be computed via an ensemble-based method as EnKF (Evensen, 2003)
 85 or its variants, EnKS (Evensen, 2003), EnHF (Liu et al., 2008), or 4DEnVAR (Liu et al.,
 86 2008) for instance.

87 2.1 Shrinkage-based Ensemble Kalman Filter

88 A more robust family of covariance estimators for the case $n \gg N$ are the shrink-
 89 age based estimators (Touloumis, 2015; Couillet & McKay, 2014). This kind of estimators
 90 have the form (Ledoit & Wolf, 2018):

$$91 \quad \mathbf{B} \approx \hat{\mathbf{B}}(\alpha) = \alpha \cdot \mathbf{T} + (1 - \alpha) \cdot \mathbf{P}^b \in \mathbb{R}^{n \times n}, \quad (5)$$

92 where $\alpha \in [0, 1]$, and $\mathbf{T} \in \mathbb{R}^{n \times n}$ is a user-defined matrix. The value of α is chosen to
 93 minimize

$$94 \quad \alpha^* = \arg \min_{\alpha} \mathbb{E} \left[\left\| \mathbf{B} - \hat{\mathbf{B}}(\alpha) \right\|_F^2 \right], \quad (6)$$

95 where $\|\bullet\|_F$ represents the Frobenius norm. A close formulation to calculate the weight
 96 value α using a general target matrix \mathbf{T}_{KA} is proposed in (Stoica et al., 2008; Zhu et al.,
 97 2011) (hereafter KA estimator),

$$98 \quad \hat{\mathbf{B}}_{KA} = \alpha_{KA} \cdot \mathbf{T}_{KA} + (1 - \alpha_{KA}) \cdot \mathbf{P}^b \in \mathbb{R}^{n \times n}, \quad (7a)$$

99 with

$$100 \quad \alpha_{KA} = \min \left(\frac{\frac{1}{N^2} \cdot \sum_{i=1}^N \|\Delta \mathbf{x}^{[e]}\|^4 - \frac{1}{N} \cdot \|\mathbf{P}^b\|^2}{\|\mathbf{P}^b - \mathbf{T}_{KA}\|^2}, 1 \right). \quad (7b)$$

101 This general target matrix enables the incorporation of *prior* information about the sys-
 102 tem into the error covariance matrix. Additionally, the KA estimator does not make any
 103 distributional assumptions, thus can also be used for non-gaussian covariance matrix es-
 104 timation (Zhu et al., 2011). An implementation of the EnKF can be obtained using the
 105 KA estimator, known as EnKF-KA (Lopez-Restrepo et al., 2021):

$$106 \quad \mathbf{X}^a = \mathbf{X}^b + \hat{\mathbf{B}}_{KA} \cdot \mathbf{H}^T \cdot [\mathbf{R} + \mathbf{H} \cdot \hat{\mathbf{B}}_{KA} \cdot \mathbf{H}^T] \cdot \mathbf{D},$$

107 where \mathbf{X}^a is the analysis ensemble, \mathbf{H} is the linear (or linearized) output operator, and
 108 the e -th column of the innovation matrix on the synthetic observations $\mathbf{D} \in \mathbb{R}^{n \times N}$ reads
 109 $\mathbf{d}^{[e]} = \mathbf{y} + \boldsymbol{\epsilon}^{[e]} - \mathcal{H}(\mathbf{x}^{b[e]}) \in \mathbb{R}^{m \times 1}$, with $\boldsymbol{\epsilon}^{[e]} \sim \mathcal{N}(\mathbf{0}, \mathbf{R})$. In Lopez-Restrepo et al.(2021),
 110 it is shown than incorporating *prior* information of the system in the data assimilation
 111 process can outperforms the EnKF when $n \gg N$, and when there are errors in the model
 112 specifications.

113 2.2 Ensemble time-local \mathbf{H}_∞ filter

114 One of the most widely used robust filter is the H_∞ Filter (HF) (Hassibi et al., 2000).
 115 The HF is based on the criterion of minimizing the supremum of the L_2 norm of the un-
 116 certainty sources (Han et al., 2009). The HF ensures that the total energy of the esti-
 117 mation errors, is not larger than the uncertainty energy times a factor $1/\gamma$:

$$118 \sum_{t=0}^M \|\mathbf{x}_t^t - \mathbf{x}_t^a\|_{\mathbf{S}_t}^2 \leq \frac{1}{\gamma} \left(\|\mathbf{x}_0^t - \mathbf{x}_0^a\|_{\boldsymbol{\Delta}_0^{-1}}^2 + \sum_{t=0}^M \|\mathbf{u}_t\|_{\mathbf{Q}_t^{-1}}^2 + \sum_{t=0}^M \|\mathbf{v}_t\|_{\mathbf{R}_t^{-1}}^2 \right), \quad (8)$$

119 where \mathbf{x}^t is the true state, \mathbf{x}^a is the analysis state, \mathbf{S} is a user-chosen matrix of weights,
 120 \mathbf{u} and \mathbf{v} are the model and observation uncertainty respectively, $\boldsymbol{\Delta}_0$, \mathbf{Q} and \mathbf{R} are the
 121 uncertainty weighting matrices with respect to the initial conditions, model error and
 122 observations error, and M is the data assimilation windows length (Luo & Hoteit, 2011).
 123 To solve (8), the cost function \mathcal{J}^{HF} is defined as:

$$124 \mathcal{J}^{\text{HF}} = \frac{\sum_{t=0}^M \|\mathbf{x}_t^t - \mathbf{x}_t^a\|_{\mathbf{S}_t}^2}{\|\mathbf{x}_0^t - \mathbf{x}_0^a\|_{\boldsymbol{\Delta}_0^{-1}}^2 + \sum_{t=0}^M \|\mathbf{u}_t\|_{\mathbf{Q}_t^{-1}}^2 + \sum_{t=0}^M \|\mathbf{v}_t\|_{\mathbf{R}_t^{-1}}^2}. \quad (9)$$

125 Then inequality (8) is equivalent to $\mathcal{J}^{\text{HF}} \leq \frac{1}{\gamma}$. Let γ^* be the value such that:

$$126 \frac{1}{\gamma^*} = \inf_{\{\mathbf{x}_t^a\}} \sup_{\mathbf{x}_0, \{\mathbf{u}_t\}, \{\mathbf{v}_t\}} \mathcal{J}^{\text{HF}}, t \leq M, \quad (10)$$

127 the optimal HF is then achieved when $\gamma = \gamma^*$. In this formulation, the evaluation of
 128 γ^* is an application of the minimax rule (Berger, 1985), a strategy that aims to provide
 129 robust estimates and is different from its Bayesian counterpart (Luo & Hoteit, 2011). An
 130 Ensemble-based HF implementation for a nonlinear DA problem is the Ensemble time-
 131 local \mathbf{H}_∞ filter (EnLTHF) proposed by (Luo & Hoteit, 2011). In the EnLTHF a local
 132 cost function is proposed:

$$133 \mathcal{J}_t^{\text{HF}} = \frac{\|\mathbf{x}_t^t - \mathbf{x}_t^a\|_{\mathbf{S}_t}^2}{\|\mathbf{x}_0^t - \mathbf{x}_0^a\|_{\boldsymbol{\Delta}_0^{-1}}^2 + \|\mathbf{u}_t\|_{\mathbf{Q}_t^{-1}}^2 + \|\mathbf{v}_t\|_{\mathbf{R}_t^{-1}}^2}. \quad (11)$$

134 The local performance level γ_t satisfies:

$$135 \frac{1}{\gamma_t} \geq \frac{1}{\gamma_t^*} = \inf_{\{\mathbf{x}_t^a\}} \sup_{\mathbf{x}_0, \{\mathbf{u}_t\}, \{\mathbf{v}_t\}} \mathcal{J}_t^{\text{HF}}, \quad (12)$$

136 The EnLTHF can be expressed in terms of the EnKF algorithm using the notation of
 137 (Luo & Hoteit, 2011):

$$138 [\mathbf{P}_t^a, \mathbf{K}_t] = \text{EnKF}(\mathbf{x}_t^a, \mathbf{Q}_t, \mathbf{H}), \quad (13a)$$

$$139 \mathbf{G}_t = [\mathbf{I}_m - \gamma_t \cdot \mathbf{P}_t^a \cdot \mathbf{S}_t]^{-1} \cdot \mathbf{K}_t, \quad (13b)$$

$$140 \mathbf{x}_t^{a(i)} = \mathbf{x}_t^{b(i)} + \mathbf{G}_t \cdot [\mathbf{y}_t - \mathbf{H}_t \cdot \mathbf{x}_t^{b(i)} + \mathbf{v}_t^i], \quad (13c)$$

$$141 \mathbf{x}_t^a = \left(\sum_{i=1}^N \mathbf{x}_t^{a(i)} \right) / N, \quad (13d)$$

$$142 (\boldsymbol{\Delta}_t^a)^{-1} = (\mathbf{P}_t^a)^{-1} - \gamma_t \cdot \mathbf{S}_t, \quad (13e)$$

143 subject to the constraint

$$144 (\boldsymbol{\Delta}_t^a)^{-1} = (\mathbf{P}_t^a)^{-1} - \gamma_t \cdot \mathbf{S}_t \geq \mathbf{0}, \quad (13f)$$

145 where the operator $\text{EnKF}(\cdot, \cdot, \cdot)$ means that \mathbf{P}_t^a and \mathbf{K}_t are obtained through the EnKF.

3 Robust Shrinkage-based Ensemble Kalman Filter

3.1 Adaptive inflation

A particular issue with ensemble-based DA algorithms is the covariance undersampling. Undersampling leads to further problems such as the ensemble collapse to an overconfident, but incorrect state, or even filter divergence (Anderson, 2001). The covariance inflation artificially increases uncertainties in the background covariance avoiding the underestimation of uncertainties, and undersampling (Belsky & Mitchell, 2018). The magnitude of the inflation depends to a large degree on each system and application (Houtekamer & Zhang, 2016).

In (13e), the presence of the extra term $-\gamma_t \cdot \mathbf{S}_t$ inflates the EnKF covariance matrix. In this way, it is possible to interpret the EnTLHF as an EnKF formulation with a specific value of inflation. This implies a theoretical and solid background to construct robust filters. Consider the case where $\mathbf{S} = \mathbf{I}_n$, that corresponds with an inflation of the analysis covariance matrix eigenvalues. To satisfy the constraint (13f), or what is equivalent, to make $(\Delta_t^a)^{-1}$ semi-definite positive, consider the SVD decomposition of \mathbf{P}_t^a

$$\mathbf{P}_t^a = \mathbf{V}_t \cdot \Sigma_t \cdot \mathbf{U}_t, \quad (14)$$

where $\Sigma_t = \text{diag}(\sigma_{t,1}, \dots, \sigma_{t,n})$ is a diagonal matrix with all the eigenvalues of \mathbf{P}_t^a in descending order, that is, $\sigma_{t,1} \geq \sigma_{t,2} \geq \dots \geq \sigma_{t,n}$ and γ_t is a variable that satisfies

$$\sigma_{t,1}^{-1} - \gamma_t \geq 0,$$

that corresponds with

$$\gamma_t \leq \frac{1}{\sigma_{t,1}},$$

guaranteeing that $(\Delta_t^a)^{-1}$ is semi-definite positive. It is convenient to introduce a performance level coefficient (PLC) c by defining

$$\gamma_t \leq \frac{c}{\sigma_{t,1}}. \quad (15)$$

In contrast to conventional inflation schemes, γ_t is adaptive in time even for a fixed c value, and it is directly related with the analysis covariance matrix.

3.2 EnTLHF-KA

According to sections 2.2 and 3.1, with a specific structure and inflation value, it is possible to obtain a robust version of the EnKF. Although the EnTLHF has shown to have a better performance than the EnKF in scenarios with high uncertainty (Luo & Hoteit, 2011; Altaf et al., 2013; Triantafyllou et al., 2013), the limitations of the EnKF with respect to the ensemble size and the ensemble normality distribution are inherited in its robust version. When the ensemble size is small $N \ll n$, sampling errors can have impact on the quality of covariances matrix estimation causing problems such as filter divergence and spurious correlations (Evensen, 2003; Houtekamer & Zhang, 2016). Even though many localization techniques have been developed to mitigate those problems, it usually prohibits its implementation in high dimensional applications (Sakov & Bertino, 2011). The shrinkage-covariance estimator methods have shown a better performance than the classical sampling covariance matrix in scenarios with small ensemble size and non-gaussianities (Chen et al., 2009; E. D. Nino-Ruiz & Sandu, 2015, 2017; Ledoit & Wolf, 2018). We propose a robust implementation of the EnKF-KA shrinkage-based method following the principles of the EnTLHF and the adaptive inflation denoted EnTLHF-KA. The EnTLHF-KA can be obtained similarly to the EnLTHF by taking

189 as base the EnKF-KA:

$$190 \quad \left[\hat{\mathbf{B}}_{KA}^a, \mathbf{K}_t \right] = \text{EnKF-KA}(\mathbf{x}_t^a, \mathbf{T}_{KA}, \mathbf{H}), \quad (16a)$$

$$191 \quad \mathbf{G}_t = \left[\mathbf{I}_m - \gamma_t \cdot \hat{\mathbf{B}}_{KA}^a \cdot \mathbf{S}_t \right]^{-1} \cdot \mathbf{K}_t, \quad (16b)$$

$$192 \quad \mathbf{x}_t^{a(i)} = \mathbf{x}_t^{b(i)} + \mathbf{G}_t \cdot [\mathbf{y}_t - \mathbf{H}_t \cdot \mathbf{x}_t^{b(i)} + \mathbf{v}_t^i], \quad (16c)$$

$$193 \quad \mathbf{x}_t^a = \left(\sum_{i=1}^N \mathbf{x}_t^{a(i)} \right) / N, \quad (16d)$$

194 where the operator EnKF-KA(\cdot, \cdot, \cdot) represents the EnKF-KA shrinkage-based method
 195 (see Section 2.1). For an specific PLC, the inflation value is obtained using (15).

196 4 Results and discussion

197 4.1 Numerical experiments

198 The Lorenz-96 is one of the most used benchmarks for testing data assimilation al-
 199 gorithms. The model is highly non-linear and with a strong relationship between the states.
 200 The Lorenz-96 dynamics are described by: (Lorenz & Emanuel, 1998; Gottwald & Mel-
 201 bourne, 2005):

$$202 \quad \frac{dx_j}{dt} = \begin{cases} (x_2 - x_{n-1}) \cdot x_n - x_1 + F & \text{for } j = 1, \\ (x_{j+1} - x_{j-2}) \cdot x_{j-1} - x_j + F & \text{for } 2 \leq j \leq n-1, \\ (x_1 - x_{n-2}) \cdot x_{n-1} - x_n + F & \text{for } j = n, \end{cases} \quad (17)$$

203 where n is the state number chosen as 40, and F is the external force. For consistency,
 204 periodic boundary conditions are assumed. We take the next considerations for the nu-
 205 merical experiments:

- 206 • The assimilation window consist of $M = 500$ observations.
- 207 • The number of observed components is $m = 20$, representing and 50% of the model
 208 components.
- The observation statistics are associated with the Gaussian distribution,

$$\mathbf{y}_t \sim \mathcal{N}(\mathbf{H} \cdot \mathbf{x}_t^a, \rho_o^2 \cdot \mathbf{I}), \text{ for } 1 \leq t \leq M, \quad (18)$$

209 where $\rho_o = 0.001$, and \mathbf{H} is a linear operator that randomly chooses the m ob-
 210 served components.

- 211 • To avoid random fluctuations, each experiment is repeated 20 times ($L = 20$).
- 212 • We compare the performance and robustness of the EnTLHF-KA against the non-
 213 robust methods EnKF and EnKF-KA, and the robust method EnTLHF.
- 214 • We take the Root-Mean-Square-Error (RMSE) of L experiments as a measure of
 215 performance,

$$216 \quad \text{RMSE} = \frac{1}{L} \cdot \sum_{l=1}^L \left(\sqrt{\frac{1}{M} \cdot \sum_{t=1}^M \left([\mathbf{x}_t^* - \mathbf{x}_t^a]^T \cdot [\mathbf{x}_t^* - \mathbf{x}_t^a] \right)^2} \right). \quad (19)$$

- 217 • We choice a PLC value $c = 0.5$ for all the experiments, following Luo and Hoteit(2011).
 218 Other c values have been tested (not reported here), but no performance improve-
 219 ments were obtained.

220 4.2 Robustness against Ensemble members

221 When the state dimension is large, it is important to test the performance with rel-
 222 ative small ensemble sizes. We evaluate both the accuracy and the robustness of the EnTLHF-
 223 KA with respect to the ensemble size. For this case we set the observation error $\delta = 1 \times 10^{-3}$,

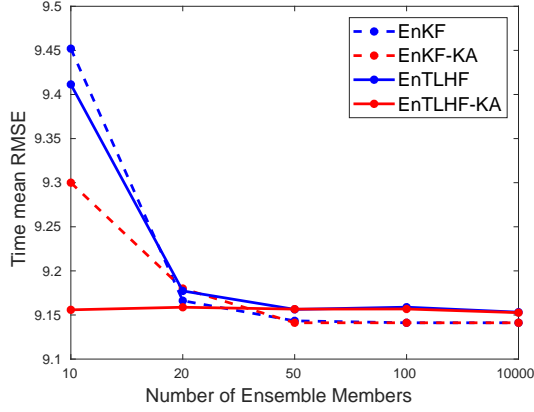


Figure 1. Error evaluation of the robust and non-robust methods respect to the ensemble member number.

224 the observation frequency $f = 1$, and the external force $F = 8$. The ensemble size $N \in$
 225 $[10, 20, 50, 100, 1000]$. Figure 1 presents the RMSE value for those values of N .

226 The EnTLHF-KA has more constant RMSE values for different N . The other meth-
 227 ods present variation in its performance when the ensemble size changes. In general, the
 228 RMSE values decrease for larger N values for all the methods. For $N = 10$, the EnTLHF-
 229 KA presents a superior performance compared to the others, followed by the EnKF-KA.
 230 This behavior is attributed to the shrinkage-based estimator used in both methods, that
 231 have shown a better covariance estimation when $N \ll n$ (E. D. Nino-Ruiz & Sandu,
 232 2017; Lopez-Restrepo et al., 2021). However, the adaptive inflation factor of the EnTLHF,
 233 and the ENTLHF-KA improves these methods' performance against its non-robust coun-
 234 terpart. For larger ensemble size, both EnTLHF-KA and EnKF-KA tend to converge
 235 to the EnTLHF and EnKF respectively, since the sampling ensemble matrix represents
 236 a good estimator for the covariance matrix and $\hat{\mathbf{B}}_{KA}$ converge to \mathbf{P}^a . Due to the good
 237 estimation of \mathbf{B} by \mathbf{P}^a , and all the EnKF assumptions are satisfied, the non-robust meth-
 238 ods present lower RMSE value for large ensemble size. This example clarifies the differ-
 239 ent advantages and disadvantages of the robust approach compared to the optimal ap-
 240 proach. Although the EnTLHF-KA performance is not the best in all the scenarios, its
 241 robustness allows it to have low RMSE values in all the scenarios.

242 4.3 Robustness against observation error

243 Figure 2 shows the RMSE value when $\delta \in [1 \times 10^{-4}, 1 \times 10^{-3}, 1 \times 10^{-2}, 1 \times 10^{-1}]$.
 244 The other model parameters are: $N = 20$, $f = 1$, and $F = 8$. The idea now is to eval-
 245 uate the impact of the observation error in the new robust EnTLHF-KA. It can be seen
 246 that the performance of the non-robust methods is affected by the increase of the ob-
 247 servation error, causing divergence of the EnKF-KA. This kind of behavior is one of the
 248 main reasons for the development of the new robust techniques (Rao et al., 2017). The
 249 observation error's impact is much lower in the robust methods, and the performance
 250 is almost constant, especially in the EnTLHF-KA. When $\delta = 1 \times 10^{-4}$, the EnKF and
 251 the EnKF-KA perform better than its robust counterpart, but the robust filters hold a
 252 good performance even for large observation errors.

253 4.4 Robustness against model errors

254 To evaluate the EnTLHF-KA robustness respect to model errors, we compare the
 255 method's performance when $F \in [6, 7, 8, 9, 10]$. $F = 8$ corresponds with the assump-

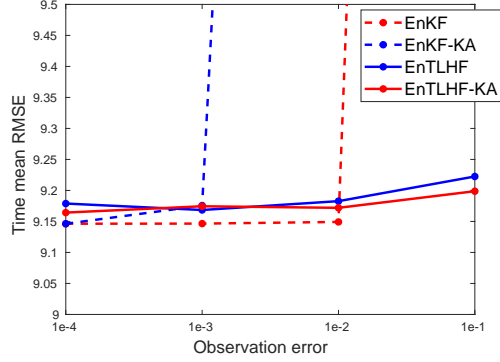


Figure 2. Error evaluation of the robust and non-robust methods respect to the observation error.

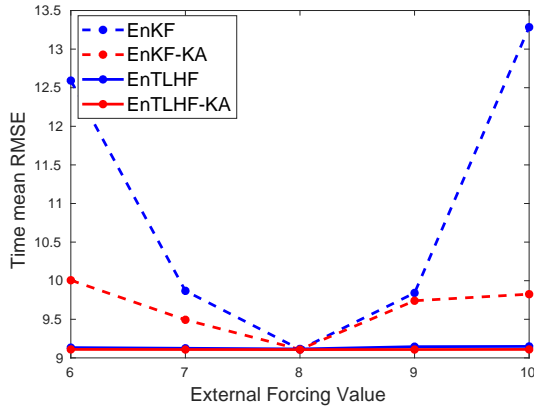


Figure 3. Error evaluation of the robust and non-robust methods respect errors in the model.

256 tion of a perfect model. Figure 3 presents the RMSE value for each F value and the com-
 257 parison among the four filters. The RMSE values remain almost constant for both ro-
 258 bust filters, with smaller values for the EnTLHF-KA. The adaptive inflation makes the
 259 analysis covariance matrix larger in the robust filters that in its non-robust counterpart,
 260 given the same background covariance. Consequently, the EnTLHF and the EnTLHF-
 261 KA put more weight in the observations, convenient when there are larger model errors.

262 4.5 Robustness against ensemble distribution

263 The standard EnKF assumes that the ensemble state has a Gaussian distribution.
 264 This assumption is especially essential because the state covariance \mathbf{B} is approximated
 265 by the ensemble sample covariance \mathbf{P}^b . Although the ensemble at t_0 is Gaussian, non-
 266 linearities in the model dynamics can modify the ensemble distribution, causing the ap-
 267 proximation of \mathbf{B} by \mathbf{P}^b to lose accuracy. Figure 4 presents an evaluation of the ensemble
 268 distribution for different times steps using the Lorenz-96 model. We use the Shapiro-
 269 Wilk to evaluate the gaussianity of each state variable (Shapiro & Wilk, 1965). We take
 270 an initial Gaussian ensemble of 100 members as reference. After 15-time steps, some vari-
 271 ables begin to change its initial distribution, and after 30-time steps, the Gaussian as-
 272 sumption is not valid anymore for the ensemble.

273 We perform different experiments varying the observation frequency or the num-
 274 ber of time steps between two available observations. Figure 5 shows the time averaged

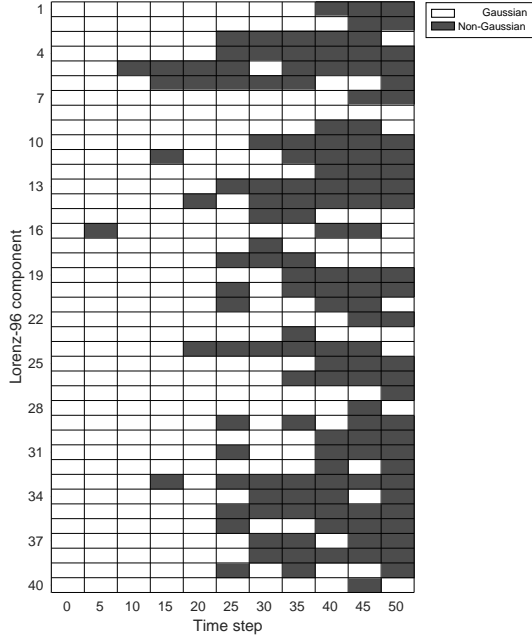


Figure 4. Shapiro-Wilk test for each Lorenz component at different time step. The ensemble size is 100. The white color represents that the null-hypothesis is not rejected (the ensemble for that specific variable is Gaussian). The grey color represents that the null-hypothesis is rejected (the ensemble for that specific variable is non-gaussian).

275 RMSE for the EnKF, EnKF-KA, EnTLHF and the EnTLHF-KA using a observation
 276 frequency $f \in [1, 5, 10, 20, 30, 50]$ times steps. We set an ensemble size of $N = 20$, an
 277 observation error of $\delta = 1 \times 10^{-3}$, and the external force $F = 8$. The EnKF perfor-
 278 mance decreases considerably when f increases, and after the value of $f = 30$ the method
 279 diverges. This result illustrates the importance of the Gaussian distribution for obtain-
 280 ing a good representation of \mathbf{B} through \mathbf{P}^b . The adaptive inflation increases EnTLHF ro-
 281 bustness and performance, even when both EnKF and EnTLHF are using the same ap-
 282 proximation of \mathbf{B} . Nevertheless, the EnTLHF performance decrease considerably when
 283 $f = 50$. In contrast, EnKF-KA and EnTLHF-KA use a shrinkage-based estimator for
 284 \mathbf{B} . The KA estimator does not assume a Gaussian distribution, as other shrinkage-based
 285 estimators do (Ledoit & Wolf, 2018; E. D. Nino-Ruiz et al., 2021). Thus, the EnKF-KA
 286 presents better performance than EnKF for large f values, and similar error levels than
 287 EnTLH without incorporating adaptive inflation. In the case of the EnTLHF-KA, the
 288 combination of both the shrinkage-based estimator and the adaptive inflation produces
 289 high robustness and performance even when the ensemble distribution is non-gaussian.

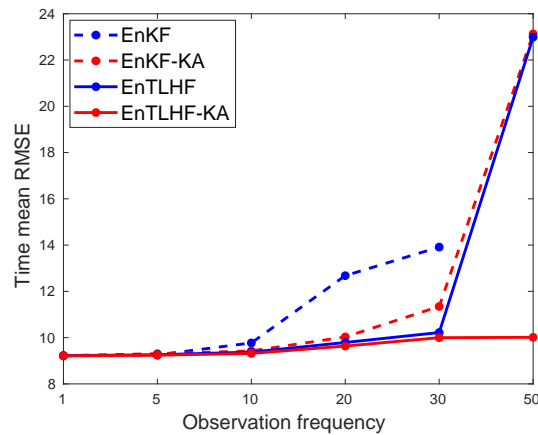


Figure 5. Error evaluation of the robust and non-robust methods respect to the observation frequency.

5 Conclusions

We propose a robust version of the shrinkage-based EnKF-KA algorithm using adaptive inflation derived from the concept of H_∞ filter (EnTLHF-KA). The EnTLHF-KA uses a covariance estimator that allows the incorporation of prior information and does not assume a Gaussian distribution in the background. Using numerical experiments, we compared the proposed method's robustness and performance against the standard EnKF, the shrinkage-based EnKF-KA, and the robust filter EnTLHF. The EnTLHF-KA has lower RMSE values in conditions with high observation error and model errors than the other methods. When the number of ensembles is small, the shrinkage estimator gives a better approximation of the background covariance matrix than the sample covariance matrix, generating lower errors in both shrinkage-based algorithm, especially in the EnTLHF-KA. The combination of the non-gaussian shrinkage estimator and the adaptive inflation grant a higher robustness to the EnTLHF-KA when the ensemble distribution is non-gaussian. All these characteristics make the EnTLHF-KA a suitable option in applications with highly non-linear models, high observation frequency, and computational restrictions in the number of ensembles.

Acknowledgments

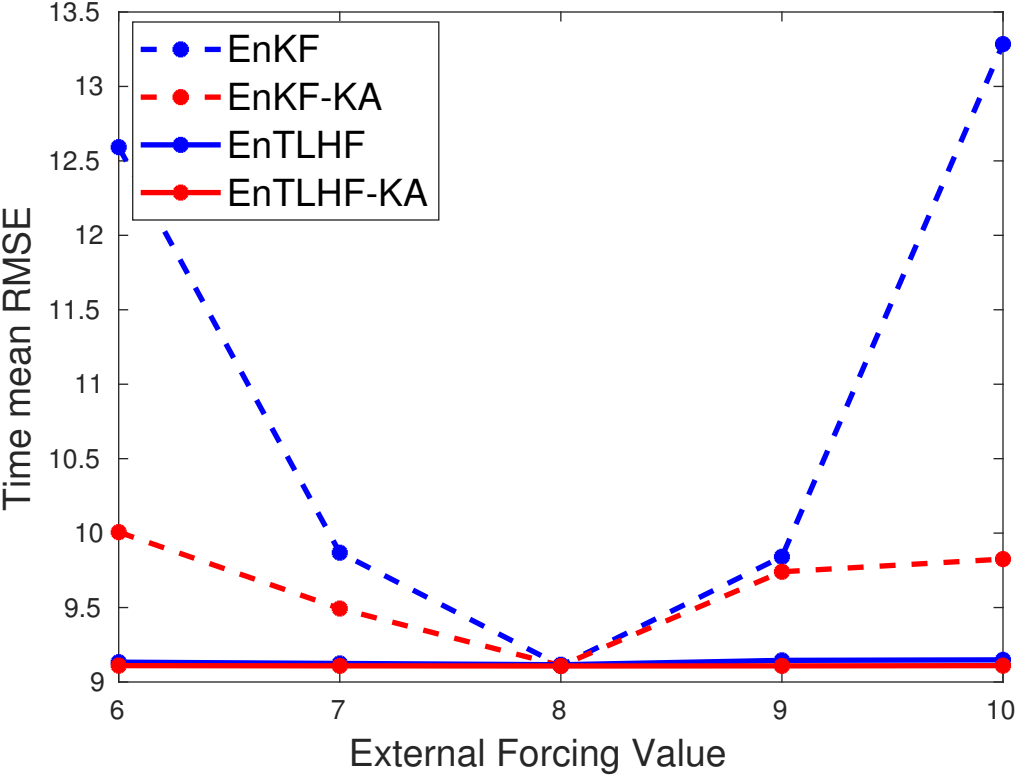
Data availability is not applicable to this article as no new data were created or analysed in this study.

References

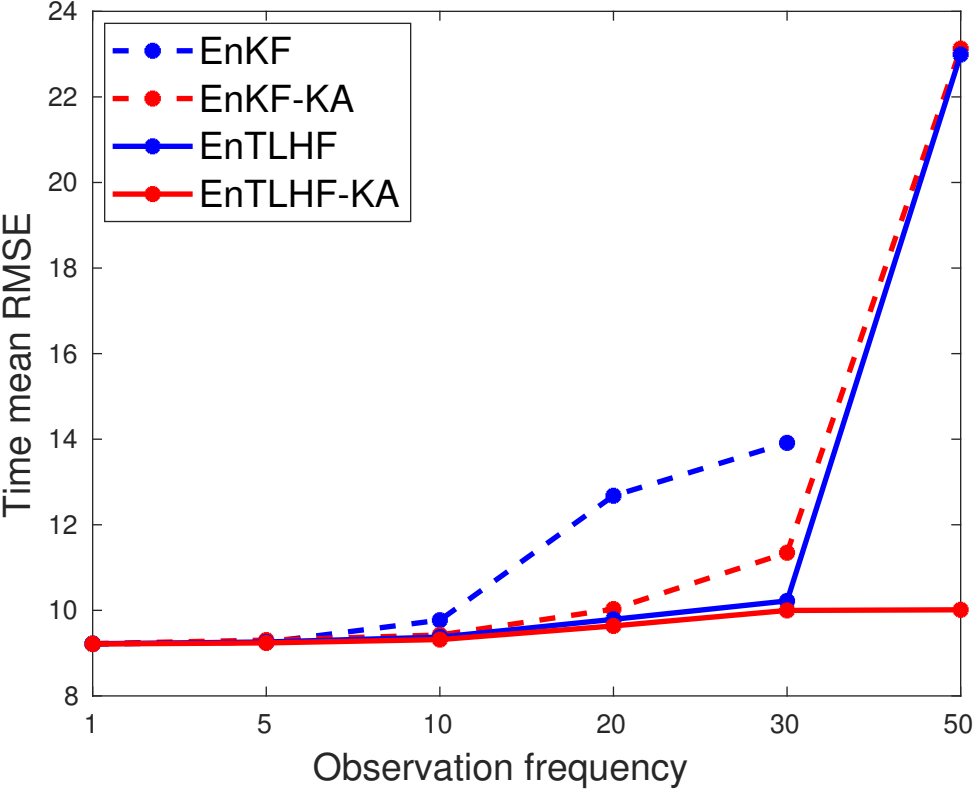
- Altaf, M. U., Butler, T., Luo, X., Dawson, C., Mayo, T., & Hoteit, I. (2013). Improving short-range ensemble kalman storm surge forecasting using robust adaptive inflation. *Monthly Weather Review*, *141*(8), 2705–2720. doi: 10.1175/MWR-D-12-00310.1
- Anderson, J. L. (2001). An ensemble adjustment kalman filter for data assimilation. *Monthly Weather Review*, *129*(12), 2884–2903. doi: 10.1175/1520-0493(2001)129<2884:AEAKFF>2.0.CO;2
- Bai, Y., Zhang, Z., Zhang, Y., & Wang, L. (2016). Inflating transform matrices to mitigate assimilation errors with robust filtering based ensemble Kalman filters. *Atmospheric Science Letters*, *17*(8), 470–478. doi: 10.1002/asl.681
- Bellsky, T., & Mitchell, L. (2018). A shadowing-based inflation scheme for ensemble

- 321 data assimilation. *Physica D: Nonlinear Phenomena*, 380-381, 1–7. Retrieved
 322 from <https://doi.org/10.1016/j.physd.2018.05.002> doi: 10.1016/j.physd
 323 .2018.05.002
- 324 Berger, J. O. (1985). *Statistical decision theory and Bayesian analysis*. New York:
 325 Springer.
- 326 Bocquet, M., Elbern, H., Eskes, H., Hirtl, M., Aabkar, R., Carmichael, G. R., ...
 327 Seigneur, C. (2015). Data assimilation in atmospheric chemistry mod-
 328 els: Current status and future prospects for coupled chemistry meteorol-
 329 ogy models. *Atmospheric Chemistry and Physics*, 15(10), 5325–5358. doi:
 330 10.5194/acp-15-5325-2015
- 331 Chen, Y., Wiesel, A., & Hero, A. O. (2009). Shrinkage estimation of high dimen-
 332 sional covariance matrices. In *2009 IEEE International Conference on Acoustics,
 333 speech and signal processing* (pp. 2937–2940).
- 334 Couillet, R., & McKay, M. (2014). Large dimensional analysis and optimization of
 335 robust shrinkage covariance matrix estimators. *Journal of Multivariate Analy-
 336 sis*, 131, 99–120.
- 337 Evensen, G. (2003). The Ensemble Kalman Filter: Theoretical formulation and
 338 practical implementation. *Ocean Dynamics*, 53(4), 343–367. doi: 10.1007/
 339 s10236-003-0036-9
- 340 Freitag, M. A., Nichols, N. K., & Budd, C. J. (2013). Resolution of sharp fronts in
 341 the presence of model error in variational data assimilation. *Quarterly Journal
 342 of the Royal Meteorological Society*, 139(672), 742–757. doi: 10.1002/qj.2002
- 343 Gottwald, G. A., & Melbourne, I. (2005). Testing for chaos in deterministic systems
 344 with noise. *Physica D: Nonlinear Phenomena*, 212(1), 100 - 110. doi: [https://
 345 doi.org/10.1016/j.physd.2005.09.011](https://doi.org/10.1016/j.physd.2005.09.011)
- 346 Han, Y., Zhang, Y., Wang, Y., Ye, S., & Fang, H. (2009). A new sequential data as-
 347 similation method. *Science in China, Series E: Technological Sciences*, 52(4),
 348 1027–1038. doi: 10.1007/s11431-008-0189-3
- 349 Hassibi, B., Kailath, T., & Sayed, A. (2000). Array algorithms for h ∞ estimation.
 350 *Automatic Control, IEEE*, 45(4), 702–706. doi: 10.1109/9.847105
- 351 Houtekamer, P. L., Mitchell, H. L., Pellerin, G., Buehner, M., Charron, M., Spacek,
 352 L., & Hansen, B. (2005). Atmospheric data assimilation with an ensemble
 353 kalman filter: Results with real observations. *Monthly weather review*, 133(3),
 354 604–620.
- 355 Houtekamer, P. L., & Zhang, F. (2016). Review of the ensemble Kalman filter for
 356 atmospheric data assimilation. *Monthly Weather Review*, 144(12), 4489–4532.
 357 doi: 10.1175/MWR-D-15-0440.1
- 358 Kalman, R. E. (1960). A new approach to linear filtering and prediction prob-
 359 lems. *Transactions of the ASME—Journal of Basic Engineering*, 82(Series D),
 360 35–45.
- 361 Lahoz, W. A., & Schneider, P. (2014). Data assimilation: Making sense of Earth Ob-
 362 servation. *Frontiers in Environmental Science*, 2(MAY), 1–28. doi: 10.3389/
 363 fenvs.2014.00016
- 364 Ledoit, O., & Wolf, M. (2018). Optimal estimation of a large-dimensional covariance
 365 matrix under stein’s loss. *Bernoulli*, 24(4B), 3791–3832.
- 366 Liu, C., Xiao, Q., & Wang, B. (2008). An ensemble-based four-dimensional varia-
 367 tional data assimilation scheme. part i: Technical formulation and preliminary
 368 test. *Monthly Weather Review*, 136(9), 3363–3373.
- 369 Lopez-Restrepo, S., Nino-Ruis, E. D., Yarce, A., Quintero, O. L., Pinel, N., Segers,
 370 A., & Heemink, A. W. (2021). An Efficient Ensemble Kalman Filter Imple-
 371 mentation Via Shrinkage Covariance Matrix Estimation: Exploiting Prior
 372 Knowledge. *Computational Geosciences*, 25, 985–1003. Retrieved from
 373 <https://doi.org/10.1007/s10596-021-10035-4>
- 374 Lorenz, E. N., & Emanuel, K. A. (1998, 02). Optimal Sites for Supplemen-
 375 tary Weather Observations: Simulation with a Small Model. *Journal*

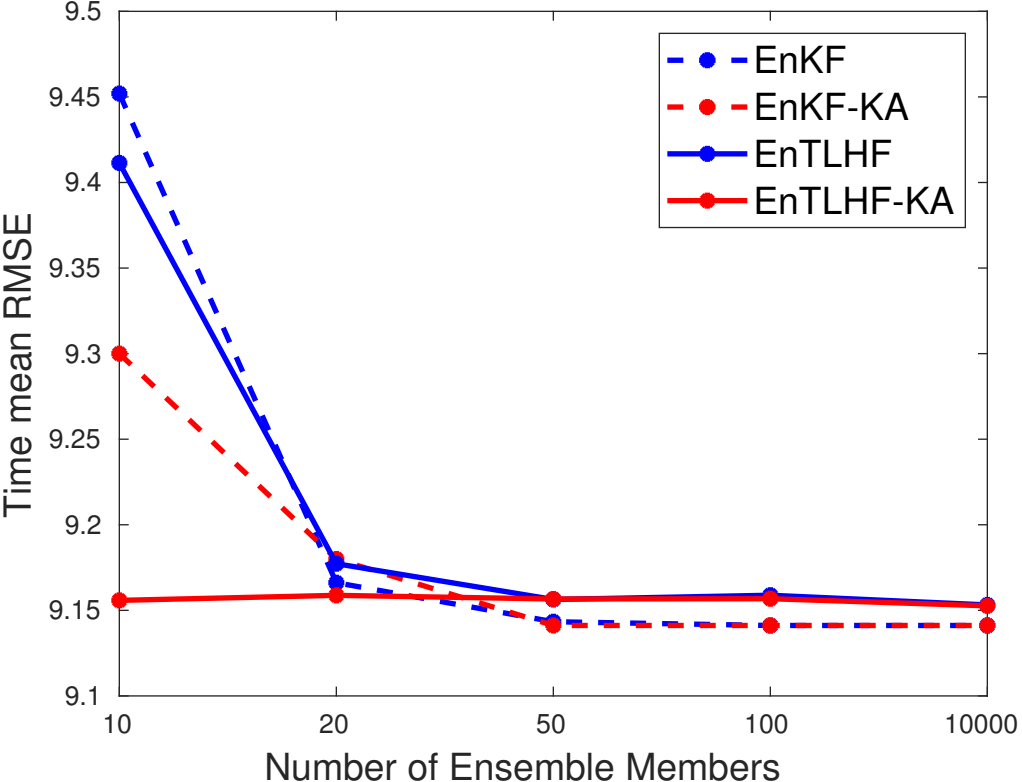
- 376 *of the Atmospheric Sciences*, 55(3), 399-414. Retrieved from [https://doi.org/10.1175/1520-0469\(1998\)055<0399:OSFSW0>2.0.CO;2](https://doi.org/10.1175/1520-0469(1998)055<0399:OSFSW0>2.0.CO;2) doi:
377
378 10.1175/1520-0469(1998)055(0399:OSFSWO)2.0.CO;2
- 379 Luo, X., & Hoteit, I. (2011). Robust Ensemble Filtering and Its Relation to Co-
380 variance Inflation in the Ensemble Kalman Filter. *Monthly Weather Review*,
381 139(12), 3938–3953. doi: 10.1175/MWR-D-10-05068.1
- 382 Nan, T.-c., & Wu, J.-c. (2017). Application of ensemble H-infinity filter in aquifer
383 characterization and comparison to ensemble Kalman filter. *Water Science and*
384 *Engineering*, 10(1), 25–35. doi: 10.1016/j.wse.2017.03.009
- 385 Nino-Ruiz, E., Cheng, H., Beltran, R., Nino-Ruiz, E. D., Cheng, H., & Beltran,
386 R. (2018). A Robust Non-Gaussian Data Assimilation Method for Highly
387 Non-Linear Models. *Atmosphere*, 9(4), 126. doi: 10.3390/atmos9040126
- 388 Nino-Ruiz, E. D., Guzman, L., & Jabba, D. (2021). An ensemble Kalman filter im-
389 plementation based on the Ledoit and Wolf covariance matrix estimator. *Jour-*
390 *nal of Computational and Applied Mathematics*, 384. Retrieved from <https://doi.org/10.1016/j.cam.2020.113163> doi: 10.1016/j.cam.2020.113163
- 391 Nino-Ruiz, E. D., & Sandu, A. (2015). Ensemble kalman filter implementations
392 based on shrinkage covariance matrix estimation. *Ocean Dynamics*, 65(11),
393 1423–1439.
- 394 Nino-Ruiz, E. D., & Sandu, A. (2017). Efficient parallel implementation of dddas
395 inference using an ensemble kalman filter with shrinkage covariance matrix
396 estimation. *Cluster Computing*, 1–11.
- 397 Rao, V., Sandu, A., Ng, M., & Nino-Ruiz, E. D. (2017). Robust data assimila-
398 tion using l1 and huber norms. *SIAM Journal on Scientific Computing*, 39(3),
399 B548–B570. doi: 10.1137/15M1045910
- 400 Roh, S., Genton, M. G., Jun, M., Szunyogh, I., & Hoteit, I. (2013, 11). Observation
401 Quality Control with a Robust Ensemble Kalman Filter. *Monthly Weather Re-*
402 *view*, 141(12), 4414-4428. doi: 10.1175/MWR-D-13-00091.1
- 403 Sakov, P., & Bertino, L. (2011). Relation between two common localisation meth-
404 ods for the EnKF. *Computational Geosciences*, 15(2), 225–237. doi: 10.1007/
405 s10596-010-9202-6
- 406 Shapiro, S., & Wilk, M. (1965, 12). An analysis of variance test for normality (com-
407 plete samples)†. *Biometrika*, 52(3-4), 591-611. Retrieved from <https://doi.org/10.1093/biomet/52.3-4.591> doi: 10.1093/biomet/52.3-4.591
- 408 Stoica, P., Li, J., Zhu, X., & Guerci, J. R. (2008). On using a priori knowledge
409 in space-time adaptive processing. *IEEE Transactions on Signal Processing*,
410 56(6), 2598–2602. doi: 10.1109/TSP.2007.914347
- 411 Touloumis, A. (2015). Nonparametric stein-type shrinkage covariance matrix esti-
412 mators in high-dimensional settings. *Computational Statistics & Data Analy-*
413 *sis*, 83, 251–261.
- 414 Triantafyllou, G., Hoteit, I., Luo, X., Tsiaras, K., & Petihakis, G. (2013). As-
415 ssuming a robust ensemble-based Kalman filter for efficient ecosystem data
416 assimilation of the Cretan Sea. *Journal of Marine Systems*, 125, 90–100. doi:
417 10.1016/j.jmarsys.2012.12.006
- 418 Yang, Y., He, H., & Xu, G. (2001). Adaptively robust filtering for kinematic geode-
419 tic positioning. *Journal of Geodesy*, 75(75), 109–116.
- 420 Zhu, X., Li, J., & Stoica, P. (2011). Knowledge-Aided Space-Time Adaptive Pro-
421 cessing. *IEEE Transaction on Aerospace And Electronic Systems*, 47(2), 1325–
422 1336.
- 423
424



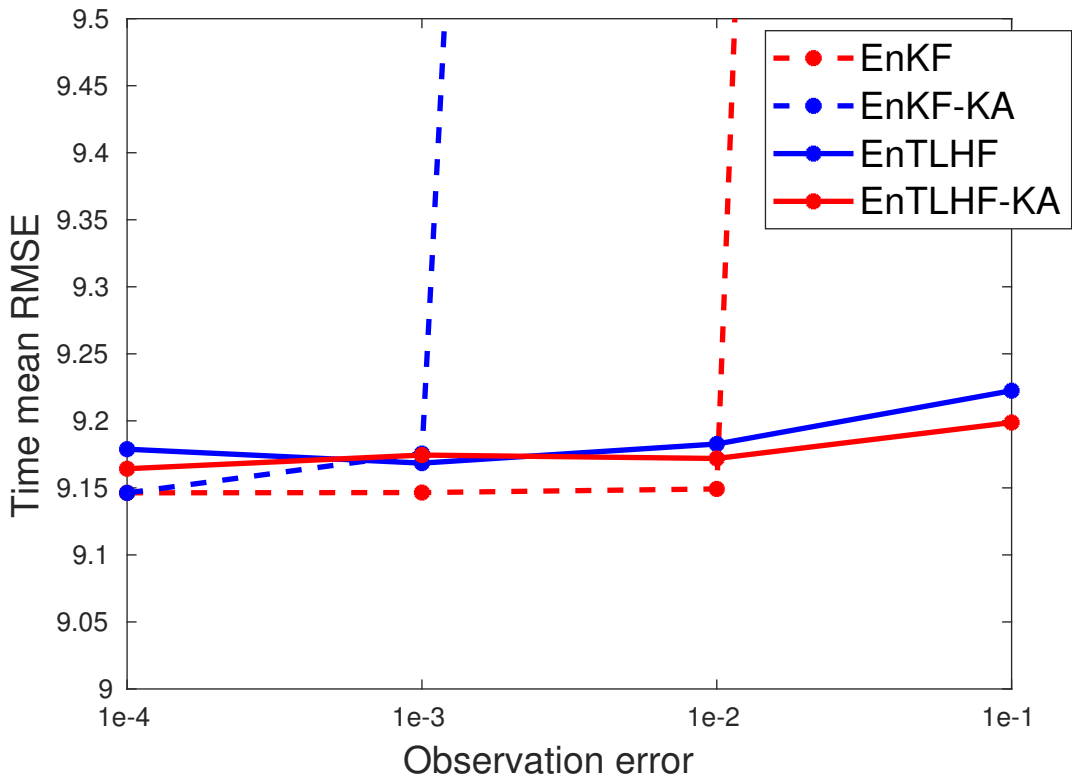
Robust_Comparison_Freq.



Robust_Comparison_N.



Robust_Comparison_sigma.



Shapiro_Matrix.

